 https://doi.org/10.24191/jeesr.v29i1.005

Clutter Simulation and Statistical Validation of Non-Stationary Maritime Radar for SISO and MIMO Systems

Nadiy Zaiaami*, Nur Emileen Abd Rashid, Suraya Zainuddin, and Nor Najwa Ismail

***Abstract*— Maritime radar systems frequently experience performance degradation due to sea clutter, which complicates the detection of small vessels and targets with low radar cross-sections. This study introduces an integrated framework for modeling, simulating, and validating maritime radar clutter using both measured and simulated data. The framework incorporates empirical parameter extraction, statistical modeling, and chunk-based simulation to replicate realistic nonstationary clutter signals. Four statistical distributions—Log-Normal, Log-Logistic, Gamma, and Weibull—are utilized to characterize the amplitude behaviour of radar clutter under varying sea and antenna conditions. Experimental measurements were obtained using Single-Input Single-Output (SISO) and Multiple-Input Multiple-Output (MIMO) radar configurations mounted on an Unmanned Surface Vehicle (USV) in a controlled basin environment. Validation is achieved through qualitative envelope comparison and quantitative error metrics, including Root Mean Square Error (RMSE). The results indicate that the Weibull distribution provides the best fit for SISO configurations across all wave heights, whereas the Gamma model performs better for MIMO configurations under increased sea roughness. These findings demonstrate the effectiveness of the proposed simulation framework in reproducing real clutter dynamics and underscore its potential to enhance maritime radar detection performance in complex sea conditions.**

***Index Terms*—Distribution fitting, GOF, Maritime clutter, MLE, RMSE, STD.**

I. INTRODUCTION

Maritime radar plays a fundamental role in navigation safety, coastal surveillance, maritime traffic monitoring, and autonomous surface vessel operations [1], [2]. Its ability to detect and track vessels under adverse weather and sea conditions makes it an indispensable sensing technology for both civilian and defence applications [3]. However, radar performance in maritime environments is severely degraded by sea clutter, which consists of unwanted echoes produced by electromagnetic scattering from the continuously varying ocean surface [4]. Sea clutter often masks weak echoes from small vessels or low radar cross-section (RCS) targets, thereby reducing detection accuracy and increasing false alarm rates [5], [6]. As maritime surveillance systems continue to evolve towards autonomous and intelligent operations, accurate characterization and modelling of sea clutter have become increasingly important for developing robust radar signal processing algorithms.

Unlike thermal noise, maritime clutter is highly non-stationary because its statistical behaviour changes continuously with environmental conditions such as wave height, wind speed, sea state, grazing angle, antenna height, and radar geometry [4]. These factors produce complex temporal fluctuations and heavy-tailed amplitude distributions that deviate significantly from Gaussian assumptions [7]. Consequently, clutter characteristics vary not only across different operating environments but also over time within the same measurement period [8]. Capturing these temporal and statistical variations is essential for evaluating radar performance, developing adaptive detection algorithms, and designing reliable Constant False Alarm Rate (CFAR) processors [9].

To represent these stochastic characteristics, numerous statistical models have been proposed for maritime clutter analysis. Classical probability density functions (PDFs), including the Log-Normal, Weibull, Gamma, and K-distributions, have been widely adopted because they provide computationally efficient representations of clutter amplitude statistics while remaining compatible with conventional radar detection theory [4]. Among these models, the Weibull and Log-Normal distributions generally provide satisfactory descriptions under relatively calm sea conditions, whereas more complex compound distributions are often required to characterise highly spiky clutter observed in rough seas [7], [10]. Although these statistical models effectively describe the marginal distribution of clutter amplitudes, they do not necessarily preserve the temporal evolution and non-stationary behaviour exhibited by measured maritime radar signals [8].

Realistic clutter simulation has therefore become an important research topic because it enables radar algorithms to be developed and evaluated without the need for repeated and costly field measurements [11]. Existing simulation approaches commonly generate synthetic clutter using predefined statistical distributions or analytical scattering models [12]. While these methods offer computational efficiency, they typically rely on

This manuscript is submitted on August 14, 2026, revised on October 5, 2026, accepted on October 5, 2026, and published on October 31, 2026.

Nadiy Zaiaami, Nur Emileen Abd Rashid, and Suraya Zainuddin are from the Faculty of Electrical Engineering, Universiti Teknologi MARA, Shah Alam.

Nor Najwa Ismail, are from the Faculty of Engineering, Universiti Putra Malaysia.

*Corresponding author
Email address: nadiyzaiaami@gmail.com

1985-5389/© 2026 The Authors. Published by UiTM Press. This is an open access article under the CC BY-NC-ND license (http://creativecommons.org/licenses/by-nc-nd/4.0/).

idealised assumptions or theoretical parameters that are not directly derived from measured radar observations [13]. As a result, many simulated datasets fail to reproduce the temporal envelope variations, heavy-tailed characteristics, and dynamic behaviour observed in real maritime environments [11]. Consequently, the simulated clutter may not accurately represent the operational conditions encountered by practical radar systems [4].

Another limitation of current studies is their primary focus on Single-Input Single-Output (SISO) radar systems. With the increasing adoption of Multiple-Input Multiple-Output (MIMO) radar for maritime surveillance, understanding clutter behaviour under multi-antenna configurations has become increasingly important [14], [15]. Compared with SISO systems, MIMO radar introduces spatial diversity, multiple observation channels, and angle-dependent scattering mechanisms that fundamentally alter clutter statistics [16]. These additional degrees of freedom influence both the temporal variability and amplitude distribution of clutter, implying that statistical models validated for SISO systems cannot be directly applied to MIMO radar without further investigation [17].

Furthermore, most existing clutter studies concentrate on statistical fitting using measured data or theoretical modelling independently, with relatively limited attention given to integrating measurement-derived statistics into a unified simulation framework [9]. In particular, few studies have simultaneously (i) preserve the non-stationary temporal characteristics extracted from measured radar data, (ii) generate long-duration realistic clutter signals suitable for radar performance evaluation, and (iii) investigate configuration-dependent statistical behaviour for both SISO and MIMO radar systems under varying sea conditions [4], [18], [19]. Addressing these limitations is essential for developing realistic clutter simulators that can support algorithm development, detector evaluation, and system performance assessment [12].

To address these challenges, this paper proposes a measurement-driven simulation framework for generating realistic non-stationary maritime radar clutter using statistical characteristics extracted directly from measured radar observations. The framework employs Hilbert-transform-based envelope analysis to estimate key temporal parameters from measured clutter signals collected using a floating platform representing an unmanned surface vehicle (USV) [20]. These measured envelope characteristics are subsequently incorporated into a chunk-based signal synthesis approach that generates long-duration clutter sequences while preserving the non-stationary behaviour observed in the original measurements [13]. The generated clutter is then statistically characterised using Log-Normal, Log-Logistic, Gamma, and Weibull distributions, with parameter estimation performed using Maximum Likelihood Estimation (MLE) [7]. Finally, the fidelity of the proposed simulation is validated through envelope comparison, probability density function fitting, and Root Mean Square Error (RMSE) analysis using both SISO and MIMO radar datasets collected under different wave heights and antenna elevations [16], [18].

The main contributions of this work are summarised as follows:

1. A measurement-driven simulation framework that synthesises realistic non-stationary maritime radar clutter using statistical parameters extracted directly from measured radar envelopes, thereby preserving temporal variability observed in real maritime environments [9], [11].
2. A unified statistical validation framework for both SISO and MIMO radar configurations, enabling systematic investigation of configuration-dependent clutter characteristics under different sea states and antenna heights [14], [18].
3. A comprehensive evaluation of statistical model suitability, demonstrating that the Weibull distribution consistently provides the best representation for SISO clutter, whereas the Gamma distribution becomes more suitable for MIMO clutter under increased sea roughness, highlighting the influence of radar configuration on clutter statistics [4], [17].

The remainder of this paper is organised as follows. Section 2 describes the proposed measurement-driven simulation framework, including parameter extraction, clutter synthesis, statistical modelling, and validation procedures. Section 3 presents and discusses the simulation and statistical validation results for both SISO and MIMO radar configurations under different sea conditions. Finally, Section 4 concludes the paper and outlines directions for future work.

II. METHODOLOGY

The proposed methodology builds upon a previously established measurement-based maritime clutter analysis, which utilized a floating platform that emulated a radar-equipped unmanned surface vehicle (USV) . In that study, maritime clutter signals were collected under controlled sea conditions at the NAHRIM facility, where antenna height and wave parameters were systematically varied. The recorded signals were processed using Hilbert-transform–based envelope extraction, and their amplitude statistics were characterised through probability density function (PDF) modelling [21]. Distribution parameters were estimated using maximum likelihood estimation (MLE), while the fitting accuracy was rigorously validated using root mean square error (RMSE) [22]. Although the previous work provided a validated statistical description of USV-based maritime clutter, it was primarily limited to analysis of measured data, where the current work extends this by transitioning from data analysis to dynamic signal synthesis [23].

In this work, the empirically derived envelope statistics are directly incorporated into a simulation engine to generate non-stationary maritime clutter signals. By embedding measured statistical characteristics into the simulation, the generated clutter preserves the amplitude variability and temporal behaviour observed in real maritime environments while enabling controlled and repeatable signal generation [24]. The framework is further extended to support both SISO and MIMO radar configurations, thereby enabling investigation of configuration-dependent clutter behaviour within a unified model. The overall methodology, illustrated in Figure 1, comprises four key stages, which are parameter extraction from measured radar data, simulation configuration, segment-based signal synthesis, and final signal reconstruction. The segment-based implementation improves computational efficiency

during high-resolution signal generation while maintaining temporal continuity and statistical consistency over long durations. This combined measurement-driven simulation framework enables the statistical validation and performance evaluation presented in the subsequent sections.

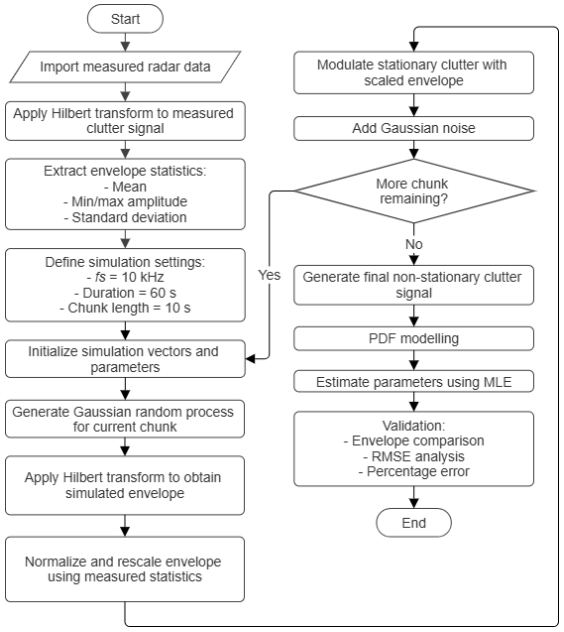


Fig. 1. Flow Chart of Simulation Process

A. Envelope Parameter Extraction from Measured Data

The simulation process begins by applying the Hilbert Transform to the measured Doppler clutter signals from the NAHRIM facility to derive the instantaneous envelope, from which three statistical parameters are extracted:

$$A_{max} = \max\big(A(t)\big) \tag{1}$$

$$A_{min} = \min\big(A(t)\big) \tag{2}$$

$$\sigma_A = \sqrt{\frac{1}{N}\sum_{i=1}^{N}(A_i - \mu_A)^2} \tag{3}$$

where A_{max} is the maximum envelope amplitude, A_{min} is the minimum envelope amplitude, and σ_A is the envelope standard deviation. The extraction of these parameters ensures that the simulation engine is not merely a random generator, but a digitally twinned model of the physical NAHRIM experimental environment [25]. These parameters define the amplitude range and fluctuation intensity of the clutter envelope, serving as direct inputs to the simulation model. In particular, σ_A represents the degree of envelope variability and reflects non-stationary behaviour induced by sea-surface dynamics. Additionally, a fixed noise standard deviation, σ_{noise} is also selected to model background system noise.

B. Chunk-Based Simulation Configuration

The simulation is implemented over 60 s duration at a sampling frequency of 10 kHz, yielding 600,000 samples. To ensure efficient memory utilization during high-resolution synthesis, a chunk-based approach is employed. The total duration is partitioned into consecutive 10-second segments, each processed independently using identical simulation parameters. The 10-second window is selected as a compromise between capturing the long-term non-stationary trends of the sea state and maintaining the short-term statistical stability required for MLE parameter estimation. To ensure seamless transitions between consecutive 10-second segments, a short overlap-add region or a smoothing window was applied at the boundaries, preventing artificial spectral leakage or discontinuities. The complete non-stationary clutter signal is then obtained by sequentially concatenating all segments, ensuring temporal continuity while maintaining computational efficiency and numerical stability.

Let N_c denote the number of samples in each simulation chunk. Each chunk is processed independently using identical procedures, and the complete nonstationary clutter signal is obtained by concatenating all chunks in temporal order. For each chunk, a zero-mean Gaussian random process is first generated to represent the initial envelope fluctuation:

$$AChunk(n) \sim N(0, {\sigma^2}_A), n = 1,2, \dots, N_c \tag{4}$$

The standard deviation, σ_A, is computed directly from the measured clutter envelope, ensuring that the simulated fluctuations align with empirical data. The key simulation parameters used in the proposed framework are summarized in Table I. These parameters define the signal generation process and ensure consistency throughout the simulation and validation stages.

TABLE I. SIMULATION PARAMETERS

Parameter	Value
Sampling frequency, f_s	10 kHz
Simulation duration, T	60 s
Chunk duration, T_c	10 s
Number of chunks, N_c	6
Samples per chunk, N	100,000
Total samples, N_{total}	600,000

C. Envelope Construction and Non-Stationary Clutter Synthesis

To extract the instantaneous envelope of the simulated process, the Hilbert Transform is applied. For a signal $x(t)$, Hilbert Transform is defined as

$$\mathcal{H}\{x(t)\} = \frac{1}{\pi}\, p.v. \int_{-\infty}^{\infty} \frac{x(\tau)}{t-\tau} d\tau \quad (5)$$

where $p.v.$ denotes the Cauchy principal value. The corresponding analytic signal is

$$z(t) = x(t) + j\mathcal{H}\{x(t)\} \quad (6)$$

and the instantaneous envelope is computed by

$$A(t) = \mid z(t) \mid = \sqrt{x(t) + \mathcal{H}\{x(t)\}} \quad (7)$$

Accordingly, the envelope of each simulated chunk is computed as:

$$A2Chunk(n) = \mid AChunk(n) + j\mathcal{H}\{AChunk(n)\} \mid \quad (8)$$

The extracted envelope is then normalised to the range $[0, 1]$ and rescaled to match the amplitude of the measured clutter envelope:

$$A_{norm}(n) = \frac{A2Chunk(n) - min(A2Chunk)}{max(A2Chunk) - min(A2Chunk)} \quad (9)$$

$$A_{scaled}(n) = A_{norm}(n)(A^m_{max} - A^m_{min}) + A^m_{min} \quad (10)$$

where *m* is referred to measuring data. This step ensures that the simulated envelope preserves the dynamic range of the measured data. Non-stationary clutter is subsequently generated by modulating a normalised stationary clutter component with the scaled envelope:

$$clutterChunk(n) = A_{scaled}(n) \times x_S(n) \quad (11)$$

where $x_S(n)$ denotes the normalized stationary clutter signal obtained by normalising the measured clutter signal to unit variance prior to envelope modulation. Finally, additive Gaussian noise, $w(n)$ is included to model background disturbances:

$$NonStatClutter(n) = clutterChunk(n) + w(n), w(n) \sim N(0, \sigma^2{}_{noise}) \quad (12)$$

All simulated chunks are concatenated sequentially to form the complete nonstationary clutter signal, ensuring temporal continuity while preserving the statistical characteristics of the measured maritime radar clutter.

D. Statistical Modelling Using Probability Density Functions (PDF)

PDF modelling is applied to statistically characterise the amplitude behaviour of maritime radar clutter using the extracted clutter envelopes. This framework enables the quantitative representation of amplitude distributions and provides a consistent basis for comparing measured and simulated data. The analysis is performed at the envelope level, as it captures the dominant amplitude fluctuations arising from sea-surface scattering. The measured radar data are segmented according to acquisition parameters, including antenna configuration (SISO/MIMO), antenna height, and sea state. Within each segment, envelope samples are treated as independent realisations of a stochastic process, and the empirical amplitude distribution is constructed.

To verify the fidelity of the simulation, the amplitude behavior is benchmarked against four candidate distributions, which are Log-Normal, Log-Logistic, Gamma, and Weibull. These distributions are chosen for their proven performance in modelling maritime clutter across varying sea conditions and grazing angles [26]. These distributions were selected to cover the wide range of clutter spikiness, from the heavy-tailed behaviour typical of high-resolution maritime radar (Log-Normal/Weibull) to the more moderate sea states (Gamma). The selected candidate distributions and their corresponding parameters are summarized in Table II.

TABLE II. PDF MODELS

Distribution	Parameters
Log-Normal	μ, σ
Log-Logistic	α, β
Gamma	k, θ
Weibull	β, η

The parameters of each candidate's probability distribution were estimated using the MLE method. MLE determines the parameter set $\hat{\theta}$that maximizes the likelihood function of the observed envelope samples, as expressed by:

$$\hat{\theta} = \arg\max_{\theta} L(\theta \mid x) \quad (13)$$

where

$$L(\theta \mid x) = \prod_{i=1}^{N} f(x_i \mid \theta) \quad (14)$$

and $f(x_i \mid \theta)$ denotes the probability density function of the selected distribution evaluated at sample x_i. The unknown distribution parameters were estimated by maximizing the likelihood function of the observed envelope samples.

For methodological consistency, the identical estimation procedure is applied to the simulated clutter envelopes generated by the proposed framework. The agreement between empirical histograms and fitted PDFs is quantified using RMSE and percentage error metrics evaluated over the full amplitude range:

$$RMSE = \sqrt{\frac{1}{N}\sum_{i=1}^{N}(P_{emp}(i) - P_{fit}(i))^2} \quad (15)$$

where P_{emp} is the empirical PDF and P_{fit} is the fitted theoretical PDF. These measures provide an objective assessment of distributional deviation and model suitability.
The combined use of temporal envelope validation and PDF-based statistical modelling ensures that both the dynamic characteristics and amplitude statistics of maritime clutter are accurately reproduced. This dual validation establishes the fidelity of the proposed framework and supports its application to radar performance evaluation, detector design, and algorithm development for both SISO and MIMO systems.

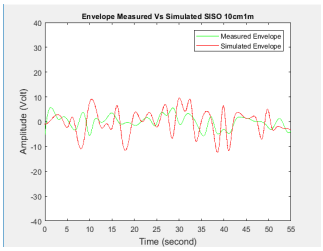
E. Validation and Performance Evaluation

The simulation framework is validated through qualitative and quantitative evaluations. Qualitative validation is performed by visually comparing the measured and simulated envelopes to assess temporal consistency and fluctuation behavior while quantitative validation is carried out using RMSE between the measured and simulated envelopes, defined as

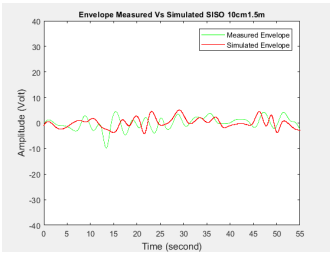
$$RMSE = \sqrt{\frac{1}{N}\sum_{i=1}^{N}(A_{measured}(i) - A_{simulated}(i))^2} \quad (16)$$

RMSE is evaluated across different sea states, antenna heights, and radar configurations to verify robustness. Together, envelope-level comparison and PDF-based error analysis confirm the proposed framework's capability to accurately reproduce both the temporal and statistical characteristics of measured maritime radar clutter.

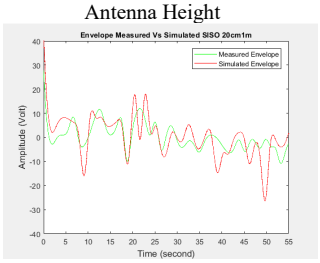
III. Results And Discussion



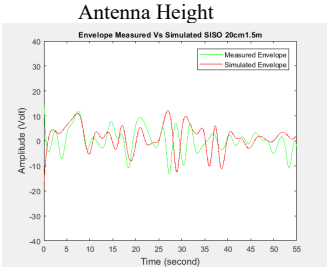
(a) 10cm Wave Height, 1m Antenna Height



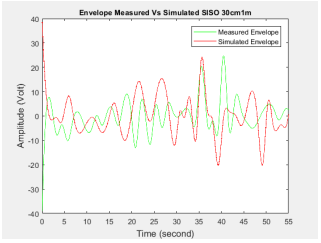
(b) 10cm Wave Height, 1.5m Antenna Height



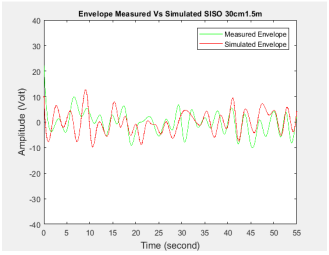
(c) 20cm Wave Height, 1m Antenna Height



(d) 20cm Wave Height, 1.5m Antenna Height



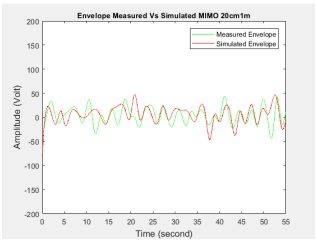
(e) 30cm Wave Height, 1m Antenna Height



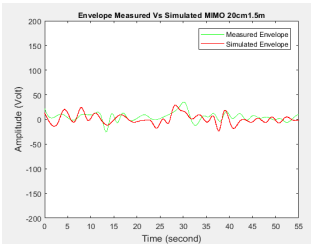
(f) 30cm Wave Height, 1.5m Antenna Height

Fig. 2. SISO Envelope of Measured and Simulated Data for 1- and 1.5-Meters Antenna

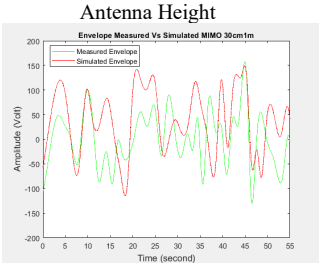
Figure 2 shows the SISO envelope of the measured and simulated signals for an antenna with lengths of 1 and 1.5m. The figure demonstrates that the simulated envelopes closely match the measured SISO clutter across all antenna heights and wave conditions. More importantly, the evolution of envelope variability with increasing wave height is evident. Although the overall temporal structure remains consistent, higher wave conditions result in more pronounced envelope intermittency, especially at the peaks. This pattern suggests that the clutter exhibits increased impulsiveness rather than uniform amplification. In addition, increasing the antenna height from 1 m to 1.5 m does not substantially change the envelope shape but does reduce the density of short-term fluctuations. This observation implies that antenna elevation primarily influences clutter stability rather than amplitude scaling, likely because it reduces sensitivity to near surface scattering effects. The simulation accurately reproduces this trend, confirming that the extracted envelope parameters effectively capture height-dependent nonstationary without the need for explicit geometric modelling.



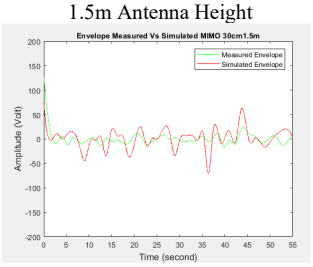
(a) 20cm Wave Height, 1m Antenna Height



(b) 20cm Wave Height, 1.5m Antenna Height



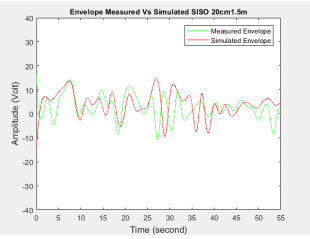
(c) 30cm Wave Height, 1m Antenna Height



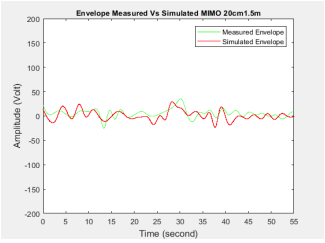
(d) 30cm Wave Height, 1.5m Antenna Height

Fig. 3. MIMO Envelope of Measured and Simulated Data for 1 and 1.5 Meters Antenna

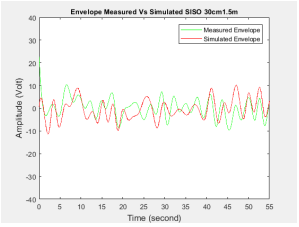
As seen in Figure 3, the MIMO configuration consistently shows a wider envelope than the SISO case, even when wave and antenna conditions are the same. This widening indicates a greater spread of envelope values over time, rather than just a higher amplitude. The effect becomes more pronounced at higher wave heights, implying that spatial diversity introduces additional fluctuation modes associated with multipath and angle-dependent scattering. Notably, the simulated MIMO envelope slightly overestimates fluctuation spread at higher wave heights. This does not indicate a modelling error; instead, it results from MIMO systems being more sensitive to weak off angle returns, which are less consistently recorded in measured data due to limited observation time. Therefore, the simulation offers a conservative estimate of clutter variability, which is useful for performance evaluation and detector stress testing.



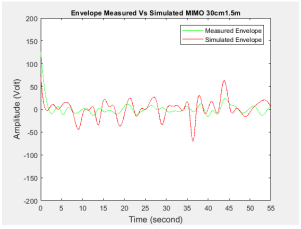
(a) SISO 20cm Wave Height, 1.5m Antenna Height



(b) MIMO 20cm Wave Height, 1.5m Antenna Height



(c) SISO 30cm Wave Height, 1.5m Antenna Height



(d) MIMO 30cm Wave Height, 1.5m Antenna Height

Fig. 4. SISO and MIMO Envelope of Measured and Simulated Data at 1 and 1.5 Meters Antenna

Figure 4 reveals how antenna configuration affects clutter statistics. SISO envelopes remain relatively compact, even at elevated wave heights, whereas MIMO envelopes display notable expansion and increased temporal variability. This distinction persists under identical environmental conditions, indicating that clutter behaviour is influenced not only by sea state but also by radar architecture. Notably, MIMO clutter transitions from primarily amplitude driven fluctuations (characteristic of SISO) to dispersion driven fluctuations, where envelope spread predominates. Consequently, a single distributional model cannot adequately represent both configurations across all conditions, necessitating the configuration specific statistical fitting addressed in Table I and II. Although the envelope comparisons in Figures 2–4 offer qualitative insight into the temporal behaviour and variability of measured and simulated clutter for both SISO and MIMO configurations, visual inspection alone does not fully characterize the underlying statistical differences. Subtle changes in envelope dispersion and intermittency, particularly under higher wave conditions and multi-antenna configurations, cannot be reliably quantified using envelope plots alone. Therefore, a quantitative statistical analysis is necessary to objectively evaluate these effects.

Tables III and IV provide a quantitative comparison of measured and simulated maritime radar clutter for SISO and MIMO configurations, respectively. In both cases, all evaluated statistical distributions produce low absolute RMSE values, indicating that the proposed data-driven simulation framework reliably reproduces the measured clutter envelopes across all examined sea states and antenna heights. This consistency supports the effectiveness of the envelope-based parameter extraction and chunk-based simulation strategy outlined in Section 2.

In the SISO configuration, Table III demonstrates that the Weibull distribution consistently yields the lowest RMSE and percentage error across all wave heights and antenna elevations. This outcome aligns with expectations, as SISO clutter is primarily influenced by surface-scale scattering mechanisms that generate moderately spiky yet statistically stable amplitude fluctuations. The sustained performance of the Weibull distribution as wave height increases suggests that, although clutter amplitude rises, the fundamental statistical structure remains largely unchanged. Another observation is the limited sensitivity of SISO clutter statistics to increased sea roughness. Even at a wave height of 30 cm, the percentage error difference between the Weibull and Gamma models remains relatively minor. This suggests that SISO clutter demonstrates only weakly heavy-tailed behaviour, and that higher sea states primarily intensify existing scattering processes rather than introducing new fluctuation modes. This result accounts for the strong visual agreement observed in the SISO envelope plots and supports the continued suitability of Weibull-based modelling for single-antenna maritime radar applications across diverse sea conditions.

In contrast, Table IV shows a fundamental change in clutter behaviour for the MIMO configuration. Although the Weibull distribution remains effective under moderate sea conditions (20 cm wave height), a distinct shift toward Gamma-dominated modelling emerges as wave height increases, especially for the 1 m antenna configuration. Across multiple high-wave scenarios, the Gamma distribution yields the lowest percentage error, outperforming the Weibull distribution by a significant margin. This shift is not readily discernible from envelope plots alone and constitutes a key, non-obvious finding of this study. The increased spatial diversity inherent in MIMO systems captures a broader spectrum of scattering contributions, including angle-dependent and multipath returns. As sea roughness intensifies, these additional scattering mechanisms introduce greater variance and dispersion in the clutter envelope, resulting in amplitude statistics that diverge from classical surface-driven Weibull behaviour. The Gamma distribution, which is more responsive to variance-dominated processes, thus becomes more suitable under these conditions. Another key finding is the moderating effect of antenna height

on MIMO clutter statistics. At higher antenna elevations, such as 1.5 meters, the Weibull distribution frequently regains dominance even when wave heights increase. This suggests that elevated antennas mitigate near-surface multipath effects and spatially average scattering contributions across the array. Consequently, MIMO clutter statistics partially revert to surface-scale behaviour, which is more effectively represented by Weibull modelling.

The results presented in Tables III and IV indicate that SISO clutter maintains statistically stable behaviour across different sea states, while MIMO clutter is significantly affected by both radar configuration and environmental conditions. While all evaluated distributions yield low RMSE values, percentage error analysis reveals substantial differences in statistical accuracy that are not apparent from RMSE alone. These findings highlight the importance of configuration-aware clutter modelling and the assessment of multiple candidate distributions when characterising maritime clutter. The framework's consistent reproduction of Weibull-dominated SISO clutter and Gamma-dominated MIMO clutter under various operating conditions demonstrates its robustness and suitability for maritime radar performance evaluation and algorithm development.

TABLE III. SISO COMPARISON OF RMSE AND PERCENTAGE ERROR MEASURED VS. SIMULATED

Parameters		STD & STD Err	PDF			
			Log-Logistic	Log-Normal	Gamma	Weibull
1-meter antenna	10 cm wave height	STD 6.8810	$RMSE_{LL}$ = 0.0033	$RMSE_{LN}$ = 0.0039	$RMSE_{G}$ = 0.0032	$RMSE_{W}$ = 0.0029
		STD Err. 0.0089	%err. =0.3339	%err. =0.3937	%err. =0.3233	%err. =0.2918±0.0089
		STDS 7.3712	$SRMSE_{LL}$ = 0.0023	$SRMSE_{LN}$ = 0.0032	$SRMSE_{G}$ = 0.0021	$SRMSE_{W}$ = 0.0016
		STD Err. 0.0095	S%err. =0.2281	S%err . =0.3166	S%err. =0.2095	S%err. =0.1561±0.0095
	20 cm wave height	STD 6.4416	$RMSE_{LL}$ = 0.0043	$RMSE_{LN}$ = 0.0051	$RMSE_{G}$ = 0.0043	$RMSE_{W}$ = 0.0040
		STD Err. 0.0083	%err. = 0.4325	%err. =0.5122	%err. = 0.4336	%err. = 0.3981±0.0083
		STDS 9.3530	$SRMSE_{LL}$ = 0.0031	$SRMSE_{LN}$ = 0.0040	$SRMSE_{G}$ = 0.0030	$SRMSE_{W}$ = 0.0026
		STDS Err. 0.0121	S%err. =0.3137	S%err. =0.4043	S%err. =0.3030	S%err. =0.2590±0.0121
	30 cm wave height	STD 9.2399	$RMSE_{LL}$ = 0.0037	$RMSE_{LN}$ = 0.0039	$RMSE_{G}$ = 0.0033	$RMSE_{W}$ = 0.0033
		STD Err. 0.0120	%err. =0.3749	%err. =0.3888	%err. =0.3261	%err. =0.2993±0.0120
		STDS 8.4633	$SRMSE_{LL}$ = 0.0022	$SRMSE_{LN}$ = 0.0024	$SRMSE_{G}$ = 0.0013	$SRMSE_{W}$ = 0.0010
		STDS Err. 0.0109	S%err. =0.2205	S%err . = 0.2355	S%err. =0.1320	S%err. =0.1049±0.0109
1.5 meters antenna	10 cm wave height	STD 8.3440	$RMSE_{LL}$ = 0.0033	$RMSE_{LN}$ = 0.0035	$RMSE_{G}$ = 0.0032	$RMSE_{W}$ = 0.0030
		STD Err. 0.0108	%err. =0.3277	%err. =0.3547	%err. =0.3160	%err. =0.3001±0.0108
		STDS 7.2368	$SRMSE_{LL}$ = 0.0016	$SRMSE_{LN}$ = 0.0022	$SRMSE_{G}$ = 0.0014	$SRMSE_{W}$ = 0.0009
		STDS Err. 0.0093	S%err. = 0.1599	S%err. = 0.2223	S%err . = 0.1368	S%err. =0.0852±0.0093
	20 cm wave height	STDS 8.1620	$RMSE_{LL}$ = 0.0032	$RMSE_{LN}$ = 0.0036	$RMSE_{G}$ = 0.0029	$RMSE_{W}$ = 0.0026
		STDS Err. 0.0106	%err. =0.3183	%err. = 0.3574	%err. =0.2875	%err. =0.2577±0.0106
		STDS 7.8446	$SRMSE_{LL}$ = 0.0024	$SRMSE_{LN}$ = 0.0030	$SRMSE_{G}$ = 0.0020	$SRMSE_{W}$ = 0.0016
		STDS Err. 0.0101	S%err. = 0.2413	S%err . =0.2993	S%err. =0.2004	S%err. =0.1577±0.0101
	30 cm wave height	STD 9.0145	$RMSE_{LL}$ = 0.0026	$RMSE_{LN}$ = 0.0032	$RMSE_{G}$ = 0.0024	$RMSE_{W}$ = 0.0021
		STD Err. 0.0117	%err. = 0.2610	%err. =0.3169	%err. =0.2407	%err. =0.2072±0.0117
		STDS 8.0345	$SRMSE_{LL}$ = 0.0018	$SRMSE_{LN}$ = 0.0028	$SRMSE_{G}$ = 0.0016	$SRMSE_{W}$ = 0.0009
		STDS Err. 0.0104	S%err. =0.1833	S%err. =0.2789	S%err. =0.1583	S%err. =0.0894±0.0104

Note: Values are presented as Mean ± Standard Error (SE) derived from the measured (STD Err) and simulated (STDS Err) signal variability.

TABLE IV. MIMO COMPARISON OF RMSE AND PERCENTAGE ERROR MEASURED VS. SIMULATED

Parameters		STD & STD Err	PDF			
			Log-Logistic	Log-Normal	Gamma	Weibull
1-meter antenna	20 cm wave height	STD 24.4411	$RMSE_{LL}$ = 0.0014	$RMSE_{LN}$ = 0.0019	$RMSE_{G}$ = 0.0008	$RMSE_{W}$ = 0.0003
		STD Err 0.0318	%err . =0.1423	%err . =0.1929	%err . =0.0774	%err . =0.0335±0.0318
		STD 21.2441	$SRMSE_{LL}$ = 0.0015	$SRMSE_{LN}$ = 0.0021	$SRMSE_{G}$ = .0008	$SRMSE_{W}$ = 0.0003
		STD Err 0.0274	S%err. =0.1453	S%err. = 0.2129	S%err. =0.0820	S%err. =0.0308±0.0274
	30 cm wave height	STD 41.6965	$RMSE_{LL}$ = 0.0013	$RMSE_{LN}$ = 0.0016	$RMSE_{G}$ = 0.0002	$RMSE_{W}$ = 0.0009
		STD Err 0.0541	%err . =0.1341	%err . =0.1584	%err . =0.0255±0.0541	%err . =0.0940
		STD 39.0495	$SRMSE_{LL}$ = 0.0014	$SRMSE_{LN}$ = 0.0022	$SRMSE_{G}$ = 0.0006	$SRMSE_{W}$ = 0.0010
		STD Err 0.0504	S%err. =0.1458	S%err . =0.2181	S%err. =0.0652±0.0504	S%err. =0.1025
1.5-meter antenna	20 cm wave height	STD 15.5768	$RMSE_{LL}$ = 0.0016	$RMSE_{LN}$ = 0.0021	$RMSE_{G}$ = 0.0011	$RMSE_{W}$ = 0.0007
		STD Err 0.0202	%err . =0.1639	%err . =0.2110	%err . =0.1053	%err . =0.0718±0.0202
		STD 20.7220	$SRMSE_{LL}$ = 0.0016	$SRMSE_{LN}$ = 0.0024	$SRMSE_{G}$ = 0.0012	$SRMSE_{W}$ = 0.0007
		STD Err 0.0268	S%err. =0.1695	S%err . =0.2429	S%err. =0.1208	S%err. = 0.0687±0.0268
	30 cm wave height	STD 18.2208	$RMSE_{LL}$ = 0.0021	$RMSE_{LN}$ = 0.0029	$RMSE_{G}$ = 0.0013	$RMSE_{W}$ = 0.0001
		STD Err 0.0237	%err . =0.2148	%err . =0.2880	%err . =0.1320	%err. = 0.0135±0.0237
		STD 37.0613	$SRMSE_{LL}$ = 0.0024	$SRMSE_{LN}$ = 0.0037	$SRMSE_{G}$ = 0.0018	$SRMSE_{W}$ = 0.0007
		STD Err 0.0478	S%err. =0.2354	S%err . =0.3708	S%err. =0.1788	S%err. =0.0719±0.0478

Note: Values are presented as Mean ± Standard Error (SE) derived from the measured (STD Err) and simulated (STDS Err) signal variability.

IV. CONCLUSION

A data-driven simulation framework was developed for modelling non-stationary maritime radar clutter using parameters extracted directly from measured radar data. The approach integrates envelope-based parameter extraction, chunk-based signal synthesis, and statistical distribution modelling to reproduce both the temporal dynamics and amplitude characteristics of real sea clutter in a computationally efficient manner. By operating at the envelope level and incorporating measured variability through Hilbert-based analysis, the framework captures non-stationary clutter behaviour without reliance on idealised assumptions.

Comprehensive validation was conducted using clutter data acquired from an unmanned surface vehicle equipped with both SISO and MIMO radar configurations under varying wave heights and antenna elevations. Envelope comparisons indicated that the simulated clutter closely follows the measured temporal structure, while quantitative evaluation using RMSE confirmed strong agreement across all tested conditions. Statistical analysis based on PDF fitting revealed that clutter behaviour is strongly dependent on radar configuration. The Weibull distribution consistently provided the best fit for SISO measurements, whereas the Gamma distribution more accurately characterised MIMO clutter under increased sea roughness, reflecting the influence of spatial diversity and multipath scattering.

The results demonstrate that the proposed simulation framework reliably reproduces configuration-dependent clutter statistics and non-stationary dynamics observed in real maritime environments. Consequently, the framework is directly applicable to practical engineering applications. Specifically, the configuration-specific statistical models can directly inform payload integration and sensor placement in autonomous vessel radar design to ensure target detection reliability under dynamic sea states. Furthermore, the generated realistic clutter envelopes provide a reliable baseline for CFAR algorithm tuning, enabling precise threshold setting to optimize detection sensitivity while mitigating false alarms during operational deployment. Future research will extend the framework to incorporate Doppler–range coupling, spatial correlation modelling for large MIMO arrays, and validation under open-sea conditions to further enhance its applicability to operational maritime radar systems.

REFERENCES

[1] J. A. S. and W. A. H. M. A. Richards, "Principles of Modern Radar: Basic principles," Jan. 2010, doi: 10.1049/SBRA021E.

[2] F. Sermi, C. Mugnai, F. Cuccoli, and L. Facheris, "A Maritime Radar Network for Surface Traffic Control Based on Service Vessels," 2013.

[3] P. Braca, S. Maresca, R. Grasso, K. Bryan, and J. Horstmann, "Maritime surveillance with multiple over-the-horizon HFSW radars: An overview of recent experimentation," *IEEE Aerospace and Electronic Systems Magazine*, vol. 30, no. 12, pp. 4–18, Dec. 2015, doi: 10.1109/MAES.2015.150004.

[4] S. Watts and L. Rosenberg, "Challenges in radar sea clutter modelling," *IET Radar, Sonar & Navigation*, vol. 16, no. 9, pp. 1403–1414, Sep. 2022, doi: 10.1049/rsn2.12272.

[5] Y. Qian *et al.*, "Maritime radar weak target detection against weather clutter based on FCOS network and dynamic ReLU," *IET Conference Proceedings*, vol. 2023, no. 47, pp. 1821–1825, Apr. 2024, doi: 10.1049/icp.2024.1360.

[6] X. Chen, J. Guan, Y. Huang, Y. Xue, and N. Liu, "Radar Signal Processing for Low-observable Marine Target-Challenges and Solutions," in *2019 IEEE International Conference on Signal, Information and Data Processing (ICSIDP)*, IEEE, Dec. 2019, pp. 1–6. doi: 10.1109/ICSIDP47821.2019.9173422.

[7] K. D. Ward, R. J. a. Tough, and P. W. Shepherd, "Modelling Sea Clutter: Correlation, Resolution and Non-Gaussian Statistics," *International Conference on Radar*, no. 449, pp. 95–99, 1997.

[8] T. R. Field and S. Haykin, "Nonlinear Dynamics of Sea Clutter," *International Journal of Navigation and Observation*, vol. 2008, pp. 1–8, 2008, doi: 10.1155/2008/863129.

[9] H. de Wind, J. Cilliers, and P. Herselman, "DataWare: Sea Clutter and Small Boat Radar Reflectivity Databases [Best of the Web," *IEEE Signal Process. Mag.*, vol. 27, no. 2, pp. 145–148, Mar. 2010, doi: 10.1109/MSP.2009.935415.

[10] P. Wu, J. Wang, and W. Wang, "A Novel Method of Small Target Detection in Sea Clutter," *ISRN Signal Processing*, vol. 2011, pp. 1–10, Jun. 2011, doi: 10.5402/2011/651790.

[11] F. Luo, Y. Feng, G. Liao, and L. Zhang, "The Dynamic Sea Clutter Simulation of Shore-Based Radar Based on Stokes Waves," *Remote Sens. (Basel).*, vol. 14, no. 16, p. 3915, Aug. 2022, doi: 10.3390/rs14163915.

[12] Y. Zhao, P.-J. Yang, X.-C. Ren, and X.-M. Zhu, "Rapid Simulation of Temporal-Spatial Correlated 3D Sea Clutter," *Int. J. Antennas Propag.*, vol. 2019, pp. 1–9, Dec. 2019, doi: 10.1155/2019/9705406.

[13] P. Zeng *et al.*, "Research on Sea Clutter Simulation Method Based on Deep Cognition of Characteristic Parameters," *Remote Sens. (Basel).*, vol. 16, no. 24, p. 4741, Dec. 2024, doi: 10.3390/rs16244741.

[14] S. Zainuddin, I. Pasya, N. E. A. Rashid, R. S. A. R. Abdullah, and A. R. Abdullah, "Performance of MIMO FMCW Radar in Detecting Small Vessels," in *2018 IEEE International RF and Microwave Conference (RFM)*, IEEE, Dec. 2018, pp. 329–332. doi: 10.1109/RFM.2018.8846475.

[15] G. Ludeno, M. Antuono, F. Soldovieri, and G. Gennarelli, "A Feasibility Study of Nearshore Bathymetry Estimation via Short-Range K-Band MIMO Radar," *Remote Sens. (Basel).*, vol. 16, no. 2, p. 261, Jan. 2024, doi: 10.3390/rs16020261.

[16] G. Gennarelli, C. Noviello, G. Ludeno, G. Esposito, F. Soldovieri, and I. Catapano, "24 GHz FMCW MIMO Radar for Marine Target Localization: A Feasibility Study," *IEEE Access*, vol. 10, pp. 68240–68256, 2022, doi: 10.1109/ACCESS.2022.3186052.

[17] X. Y.-H. Xue Yong-Hua, L. X.-Y. Li Xiu-You, and S. Y.-L. Sun Yan-Li, "Knowledge-aided target detection in sea clutter for distributed MIMO sky-wave radar," in *IET International Radar Conference 2015*, Institution of Engineering and Technology, 2015, pp. 5 .-5 . doi: 10.1049/cp.2015.1154.

[18] M. N. Zaiaami, I. Pasya, N. E. Abd. Rashid, N. Najwa Ismail, and A. R. Abdullah, "Radar Clutter Analysis Based on Sea-To-Sea Wave Propagation in SISO and SIMO Radar," in *2022 IEEE International RF and Microwave Conference (RFM)*, IEEE, Dec. 2022, pp. 1–4. doi: 10.1109/RFM56185.2022.10065227.

[19] Nadiy Zaiaami, N. E. Abd Rashid, N. N. Ismail, I. P. Ibrahim, S. A. Enche Ab Rahim, and N. A. Zalina Zakaria, "Clutter evalution of unmanned surface vehicles for maritime traffic monitoring," *Bulletin of Electrical Engineering and Informatics*, vol. 13, no. 3, pp. 1638–1646, Jun. 2024, doi: 10.11591/eei.v13i3.6836.

[20] M. Nadiy Zaiaami, N. E. Abd Rashid, N. N. Ismail, I. P. Ibrahim, S. A. Enche Ab Rahim, and N. A. Zalina Zakaria, "Clutter evalution of unmanned surface vehicles for maritime traffic monitoring," *Bulletin of Electrical Engineering and Informatics*, vol. 13, no. 3, pp. 1638–1646, Jun. 2024, doi: 10.11591/eei.v13i3.6836.

[21] S. Angelliaume, L. Rosenberg, and M. Ritchie, "Analysis of Bistatic Radar Sea Clutter Amplitude Distributions at Low Grazing Angles," in *2019 International Radar Conference (RADAR)*, IEEE, Sep. 2019, pp. 1–5. doi: 10.1109/RADAR41533.2019.171222.

[22] S. Angelliaume, L. Rosenberg, and M. Ritchie, "Modeling the Amplitude Distribution of Radar Sea Clutter," *Remote Sens. (Basel).*, vol. 11, no. 3, p. 319, Feb. 2019, doi: 10.3390/rs11030319.

[23] T. Oyedokun and M. Inggs, "Design and evaluation of a sea clutter simulator," in *2011 IEEE International Geoscience and Remote Sensing Symposium*, IEEE, Jul. 2011, pp. 2089–2092. doi: 10.1109/IGARSS.2011.6049576.

[24] S. Gogineni *et al.*, "High Fidelity RF Clutter Modeling and Simulation," *IEEE Aerospace and Electronic Systems Magazine*, vol. 37, no. 11, pp. 24–43, Nov. 2022, doi: 10.1109/MAES.2022.3208862.

[25] J. Kannanthara *et al.*, "Whole system radar modelling: Simulation and validation," *IET Radar, Sonar & Navigation*, vol. 17, no. 6, pp. 1050–1060, Jun. 2023, doi: 10.1049/rsn2.12399.

[26] R. Palama, M. S. Greco, P. Stinco, and F. Gini, "Statistical analysis of bistatic and monostatic sea clutter," *IEEE Trans. Aerosp. Electron. Syst.*, vol. 51, no. 4, pp. 3036–3054, Oct. 2015, doi: 10.1109/TAES.2015.140438.